Received: 18 December 2021 | Accepted: 27 June 2022

DOI: 10.1002/mrd.23631

Molecular Reproduction & Development

RESEARCH ARTICLE

RNA-sequencing reveals genes linked with oocyte developmental potential in bovine cumulus cells

Álvaro Martínez-Moro[1,2] | Leopoldo González-Brusi[1] | Ismael Lamas-Toranzo[1] | Elena O'Callaghan[3] | Anna Esteve-Codina[4] | Pat Lonergan[3] | Pablo Bermejo-Álvarez[1]

[1]Department of Animal Reproduction, INIA, CSIC, Madrid, Spain

[2]Embryology, IVF Spain, Madrid, Spain

[3]Agriculture and Food Science, School of Agriculture and Food Science, University College Dublin, Dublin, Ireland

[4]Functional Genomics, CNAG-CRG, Centre for Genomic Regulation, Barcelona Institute of Science and Technology, Barcelona, Spain

Correspondence
Pablo Bermejo-Álvarez, Department of Animal Reproduction, INIA-CSIC, 28040 Madrid, Spain.
Email: bermejo.pablo@inia.es

Funding information
Comunidad de Madrid; Ministerio de Economía y Competitividad, Gobierno de España, Grant/Award Numbers: AGL2017-84908-R, PID2020-117501RB-I00

Abstract

Cumulus cells provide an interesting biological material to perform analyses to understand the molecular clues determining oocyte competence. The objective of this study was to analyze the transcriptional differences between cumulus cells from oocytes exhibiting different developmental potentials following individual in vitro embryo production by RNA-seq. Cumulus cells were allocated into three groups according to the developmental potential of the oocyte following fertilization: (1) oocytes developing to blastocysts (Bl+), (2) oocytes cleaving but arresting development before the blastocyst stage (Bl−), and (3) oocytes not cleaving (Cl−). RNAseq was performed on 4 (Cl−) or 5 samples (Bl+ and Bl−) of cumulus cells pooled from 10 cumulus-oocyte complexes per group. A total of 49, 50, and 18 differentially expressed genes (DEGs) were detected in the comparisons Bl+ versus Bl−, Bl+ versus Cl− and Bl- versus Cl−, respectively, showing a fold change greater than 1.5 at an adjusted *p* value <0.05. Focussing on DEGs in cumulus cells from Bl+ group, 10 DEGs were common to both comparisons (10/49 from Bl+ vs. Bl−, 10/50 from Bl+ vs. Cl−). These DEGs correspond to 6 upregulated genes (*HBE1*, *ITGA1*, *PAPPA*, *AKAP12*, *ITGA5*, and *SLC1A4*), and 4 downregulated genes (*GSTA1*, *PSMB8*, *FMOD*, and *SFRP4*) in Bl+ compared to the other groups, from which 7 were validated by quantitative PCR (*HBE1*, *ITGA1*, *PAPPA*, *AKAP12*, *ITGA5*, *PSMB8* and *SFRP4*). These genes are involved in critical biological functions such as integrin-mediated cell adhesion, oxygen availability, IGF and Wnt signaling or PKA pathway, highlighting specific biological processes altered in incompetent in vitro maturation oocytes.

KEYWORDS

granulosa cell, integrin, in vitro maturation, oocyte quality, transcription

1 | INTRODUCTION

In vitro embryo production (IVP) enables relevant applications for cattle reproductive management, including alleviating the negative effects of heat stress (Baruselli et al., 2020) and accelerating genetic improvement, especially when combined with sexed semen and embryo genomic selection (Ferre et al., 2020). Nevertheless, the general efficiency of the IVP process remains relatively low, as only between 30% and 40% of in vitro matured oocytes reach the blastocyst stage following fertilization and culture. Reduced oocyte

competence clearly stands out as a major causative factor for the reduced developmental rates in IVP, as in vivo matured oocytes exhibit significantly higher developmental rates following in vitro fertilization (IVF) than those matured in vitro (Dieleman et al., 2002; Rizos et al., 2002; van de Leemput et al., 1999). In this context, understanding the underlying molecular regulation of oocyte competence is critical to improve IVP, but molecular analyses in oocytes are typically invasive, involve destroying the oocyte and are thus incompatible with subsequent embryo development. One solution is to use the surrounding cumulus cells as proxies of oocyte quality as they constitute an attractive matrix on which to perform molecular analyses, and are closely connected to the oocyte during growth and final maturation, serving essential metabolic and signaling functions.

Previous attempts to discover genes whose transcript abundance in cumulus cells may serve as predictor for bovine oocyte competence have been focused on comparing cumulus cells from groups of oocytes whose developmental competence was indirectly inferred by follicle size (Melo et al., 2017), the use of different in vitro maturation (IVM) media (Assidi et al., 2008), or their origin: in vivo versus in vitro (Salhab et al., 2013; Tesfaye et al., 2009), prepubertal versus adult (Bettegowda et al., 2008), or collected before versus after LH surge (Assidi et al., 2010) or at different times following FSH withdrawal (Bunel et al., 2014). Unfortunately, the candidate genes identified on the microarray-based experiments mentioned above show very poor correlation between studies. Besides, these candidates genes were not coincident with those identified on a microarray-based experiment where oocyte developmental competence was directly assessed by performing individual IVP (Bunel et al., 2015). Another study analyzing the expression of candidate genes by quantitative PCR (qPCR) in cumulus cells from oocytes showing different developmental competence also showed results discordant with microarray data (Kussano et al., 2016), indicating that the molecular signature of the developmentally competent oocyte still remains elusive.

The reasons for the lack of agreement between studies may have a biological basis, as the different classification criteria used to indirectly infer oocyte competence dealt with diverse biological processes such as follicle growth or hormonal response which may have a transcriptional effect on their own different from the sought-after transcriptional signature of developmental competence. Another possible source of inconsistency may be technical, as microarray based experiments rely on a finite number of probes that vary depending on the manufacturer. In contrast to microarray, RNA-seq provides an unbiased search for candidate transcripts and yield a higher dynamic range, ultimately leading to higher accuracy. The objective of this study was to apply RNA-seq to uncover the transcriptional differences between cumulus cells enclosing oocytes that exhibit different developmental competence. To that aim, individual IVP was performed to infer directly the developmental potential of each oocyte. Once the developmental potential of each cumulus-oocyte complexe (COC) was known, the stored cumulus cells were allocated to one of three groups according to the oocyte's developmental potential: (1) Oocytes not cleaving following IVF (Cl−), (2) oocytes cleaving but not developing to blastocysts (Bl−) and (3) oocytes developing to blastocyst (Bl+).

2 | RESULTS

To correlate cumulus cell transcription with the developmental competence of the enclosed oocyte, COCs were individually matured. Cumulus cell samples were collected from 396 individual COCs in 7 replicates. Developmental potential of each individual oocyte was assessed at 48 h postinsemination (cleavage rate 52.3%, 207 embryos cleaved) and at day 8 postinsemination (blastocyst rate 13.4%, 53 blastocysts). Once the developmental potential of each COC was known, the stored cumulus cells were allocated to one of three groups according to the oocyte's developmental potential: (1) Oocytes not cleaving following IVF (Cl−), (2) oocytes cleaving but not developing to blastocysts (Bl−) and (3) oocytes developing to blastocyst (Bl+).

RNA-seq detected the expression of 19,335 genes in bovine cumulus cells samples. Using a raw p value <0.05, inappropriate for RNA-seq data as described below, the analysis identified 1609, 1466, and 1420 differentially expressed genes (DEGs) for the comparisons Bl+ versus Bl−, Bl+ versus Cl−, and Bl− versus Cl−, respectively (Figure 1). These DEGs were narrowed down to 77, 80, and 32 DEGs for the comparisons Bl+ versus Bl−, Bl+ versus Cl−, and Bl− versus Cl−, respectively, when an adjusted p value < 0.05 was used. Such adjusted p value takes into account the data overdispersion inherently associated with RNA-seq data, yielding a more reliable result. From these subsets of DEGs obtained at an adjusted p value <0.05, 49, 50, and 15 DEGs, for the comparisons Bl+ versus Bl−, Bl+ versus Cl−, and Bl− versus Cl−, respectively, exhibited a fold change greater than 1.5 (Figure 1 and Table 1).

Enrichment analysis failed to find enriched terms in the 15 DEGs in Bl− versus Cl− comparison, but four common enrichment terms (FDR < 0.05) were found in the comparisons Bl+ versus Bl− and Bl+ versus Cl−: "integrin domain superfamily," "cell surface receptor signaling pathway," "response to organic substance," and "response to chemical." There were also terms exclusive to Bl+ versus Cl− and Bl+ versus Bl− comparisons: "Extracellular region" and "proteosomal complex" were exclusive to the Bl+ versus Cl− comparison and "anatomical structure morphogenesis," "positive regulation of cell communication," or "cell communication" were exclusive to Bl+ versus Bl− comparison.

Interaction networks allow to determine if the proteins encoded by DEGs interact directly (physical) or indirectly (functional) with each other, aiming to uncover network properties associated to developmental potential. The interaction network from DEGs in the Bl− versus Cl− comparison did not show a significant connectivity, as the observed interactions (5) were close to the expected random observations (3). In contrast, there were statistically significant relationships for DEGs in Bl+ versus Bl− and Bl+ versus Cl− comparisons. In the case of the 50 DEGs in the Bl+ versus Cl− comparison, there were 59 observed interactions versus 33 expected (Figure 2). Several clusters of genes in the interaction network coded for proteins that were related to enriched terms were selected. such as (1) extracellular matrix organization, including *PXDN*, *TNC*, *ITGA1*, *ITGA8*, and *FMOD*), (2) cytokine signaling in

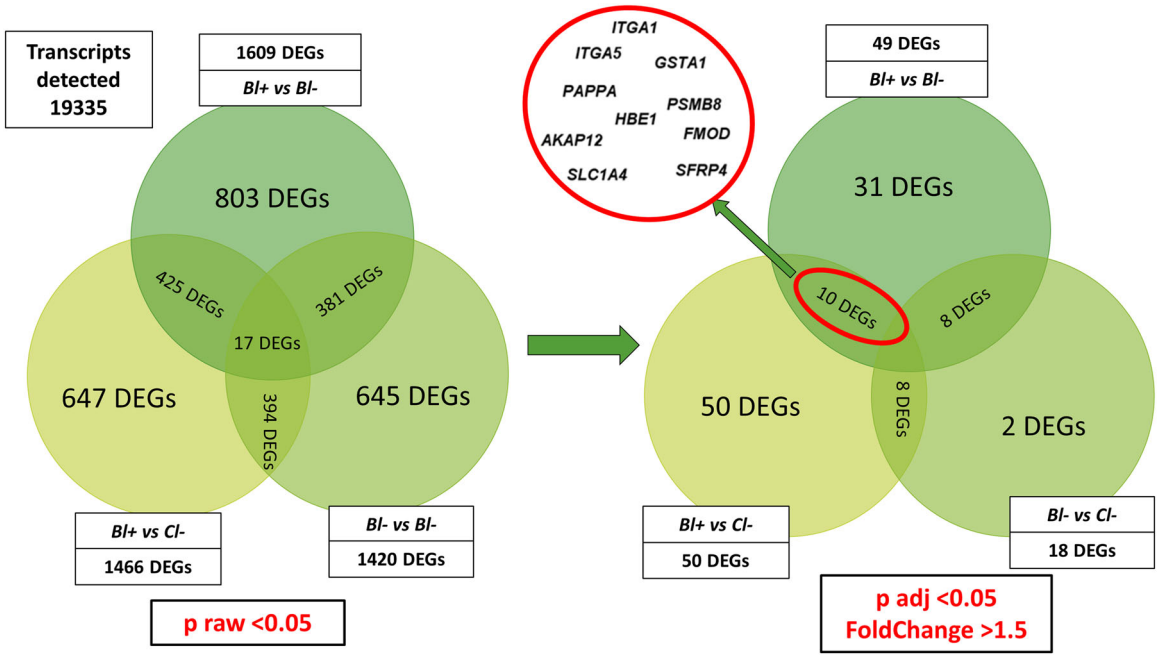

FIGURE 1 Venn diagram of differentially expressed genes (DEG) for the comparisons of the three groups exhibiting different developmental ability following IVF (Bl+, Bl−, and Cl−). Image on left shows DEG at a p raw <0.05. These lists of DEG are reduced by applying an adjusted $p < 0.05$ and a fold change greater than 1.5 (right image). 10 DEGs were common to Bl+ versus Bl− and Bl+ versus Cl− comparisons (red circle on right image)

immune system including *PSME2*, *SAMHD1*, *IFI6*, *GBP4*, *PSMB9*, *PSMB8*, *LGALS9*, *IFITM3*, *IFI35*, and *IFI27*, and (3) G alpha (q) signaling events, including *NTS*, *F2RL2*, and *HCTRC1*. Interaction analysis of the 49 DEGs in the Bl+ versus Bl− comparison observed 69 interactions versus 23 expected (Figure 2). Although the connectivity found Bl+ versus Bl− was weaker than for Bl+ versus Cl−, several nodes including *NTRK2*, *CDH17*, and *ACTN1* or *HMCN2* displayed a high number of connections.

A more stringent selection of DEGs was obtained through the three-group experimental design. Such a design constitutes a double check for DEGs potentially associated with oocyte developmental potential as both Bl+ versus Bl− and Bl+ versus Cl− comparisons contrast COCs exhibiting good developmental potential (Bl+) to COCs resulting in developmental arrest (Bl− and Cl−) (Figure 1). At an adjusted p value > 0.05 and fold change >1.5, 10 DEGs were common to both comparisons (10/49 from Bl+ vs. Bl−, 10/50 from Bl+ vs. Bl−). These DEGs correspond to 4 genes upregulated (*GSTA1*, *PSMB8*, *FMOD*, and *SFRP4*) and 6 genes downregulated (*HBE1*, *ITGA1*, *PAPPA*, *AKAP12*, *ITGA5*, and *SLC1A4*) in Bl+ compared to the other groups and none exhibited statistically significant differences in the Bl− versus Cl− comparison. Nine of those genes were selected for RNA-seq validation by qPCR, as we were unable to amplify *SLC1A4* by qPCR from cumulus cell complementary DNA (cDNA) samples at an efficiency compatible with reliable quantification. qPCR was performed using the same RNA samples than those employed for RNA-seq, so although this provides a technical validation (using different retrotranscription and technique) no validation in independent biological samples was tested. qPCR confirmed the significant differences observed by RNA-seq in both comparisons for *HBE1*, *ITGA1*, *PAPPA*, *ITGA5*, and *SFRP4*. In the case of *AKAP12* and *PSMB8* only the Bl+ versus Cl− comparison remained significant, whereas no significant difference between groups were observed for *GSTA1* and *FMOD* (Figure 3).

3 | DISCUSSION

The transcriptional analysis of individual COCs requires two critical modifications to conventional bovine IVP procedures: (1) individual IVP (iIVP) and (2) cumulus cell removal before fertilization. As a consequence of these modifications, blastocyst rates are halved compared to conventional IVP, impairing a direct application for commercial IVP. Given that we have previously observed that cumulus cell removal before IVF does not cause a significant reduction in blastocyst rate when IVP is conducted in groups (Lamas-Toranzo et al., 2019), we believe that the major cause of the reduced developmental rate is iIVP, as previously reported by others (Bunel et al., 2015). In this sense, while current methods allow performing iIVP to elucidate molecular clues of developmental competence (i.e., this experiment) further advances on iIVP are needed to be able to apply oocyte selection markers for commercial IVP purposes.

The transcriptional analysis of cumulus cells obtained from oocytes of known developmental potential has identified different biological pathways that are likely involved in oocyte quality. Among the different DEGs obtained in this analysis, integrins may be a key

TABLE 1 Differentially expressed genes at a *p* adjusted value <0.05 and fold change >1.5 at the three comparisons

	baseMean	log2FoldChange	shrunkenlfc	lfcSE	stat	filter	*p* value	padj	Fold change	Shrunken Fold change
ENSBTAG00000037815, HBE1, protein_coding	26.4787138	−2.12882978	−0.77751908	0.3854938	−5.5223451	1	3.35E-08	0.00012695	−4.37362577	−1.71418056
ENSBTAG00000012519, XDH, protein_coding	34.9303151	−1.70602939	−0.61150107	0.39614703	−4.30655603	1	1.66E-05	0.00980409	−3.26261644	−1.52784805
ENSBTAG00000002319, HMCN2, protein_coding	60.1771415	−1.64057208	−0.50575982	0.4298763	−3.81638177	0	0.00013542	0.0356707	−3.11789443	−1.41987096
ENSBTAG00000015409, STK32B, protein_coding	15.6495314	−1.55173881	−0.53294504	0.4260127	−3.64247075	0	0.00027003	0.04909611	−2.9317027	−1.44687977
ENSBTAG00000035005, protein_coding	17.6713968	−1.52954229	−0.57825979	0.3999492	−3.82434143	0	0.00013112	0.03554952	−2.88694232	−1.49304721
ENSBTAG00000000817, SYNJ2, protein_coding	48.4180788	−1.12361283	−0.55634793	0.29865507	−3.7622426	0	0.0001684	0.03880699	−2.1789194	−1.47054194
ENSBTAG00000017733, CA2, protein_coding	1232.68419	−1.09137678	−0.5943611	0.27937775	−3.90645558	1	9.37E-05	0.03011709	−2.13077282	−1.50980382
ENSBTAG00000010273, EREG, protein_coding	63.657073	−1.04827932	−0.56793004	0.28411068	−3.6896864	0	0.00022453	0.0463371	−2.06806183	−1.48239512
ENSBTAG00000016525, ITGA1, protein_coding	100.3518	−1.02332528	−0.62989844	0.23029216	−4.44359582	1	8.85E-06	0.00654253	−2.03259851	−1.54745606
ENSBTAG00000010647, NTRK2, protein_coding	44.2282193	−0.96405071	−0.5662427	0.25350133	−3.80294139	0	0.00014299	0.03649014	−1.9507795	−1.48066237
ENSBTAG00000020895, LOXL4, protein_coding	9013.3992	−0.9606973	−0.5492939	0.2537134	−3.78654545	0	0.00015276	0.03705543	−1.94625035	−1.46336931
ENSBTAG00000008814, ADGRA2, protein_coding	544.473729	−0.94162586	−0.6037932	0.2221158	−4.23934655	1	2.24E-05	0.01084811	−1.92069157	−1.519707
ENSBTAG00000002888, TMTC2, protein_coding	1371.22778	−0.92371015	−0.56201345	0.24029339	−3.84409312	0	0.000121	0.03485529	−1.89698747	−1.47632817
ENSBTAG00000018255, ACTN1, protein_coding	1406.51659	−0.91290287	−0.646985	0.19274936	−4.73621729	1	2.18E-06	0.00301075	−1.88283017	−1.56589231
ENSBTAG00000052736, protein_coding	70.0576043	−0.91195359	−0.56554114	0.23423242	−3.89337057	0	9.89E-05	0.03080768	−1.88159169	−1.47994251
ENSBTAG00000004010, PAPPA, protein_coding	705.782085	−0.89773068	−0.58690686	0.21375835	−4.19974556	1	2.67E-05	0.01231594	−1.86313302	−1.50202295
ENSBTAG00000005714, ACTC1, protein_coding	1295.44064	−0.8687399	−0.54698365	0.2328306	−3.73121023	0	0.00019056	0.0420548	−1.82606725	−1.46102782
ENSBTAG00000004375, ESRP2, pseudogene	66.9836549	−0.85983042	−0.61682149	0.19224247	−4.47263519	1	7.73E-06	0.00628409	−1.81482497	−1.5334929
ENSBTAG00000017086, GRB10, protein_coding	468.565501	−0.82402184	−0.53702793	0.21830105	−3.77470396	0	0.0001602	0.03767073	−1.77033432	−1.4509803
ENSBTAG00000014270, UNC5B, protein_coding	1451.4862	−0.80782213	−0.57019158	0.19370083	−4.17046284	0	3.04E-05	0.01313486	−1.75056682	−1.48472071
ENSBTAG00000014705, HES4, protein_coding	401.094545	−0.80463733	−0.57900276	0.18921065	−4.25260065	0	2.11E-05	0.01084811	−1.74670664	−1.49381631
ENSBTAG00000014788, AKAP12, protein_coding	3125.78806	−0.80402001	−0.56642493	0.19181549	−4.19163227	0	2.77E-05	0.01235307	−1.74595939	−1.4808494
ENSBTAG00000013745, ITGA5, protein_coding	8536.22896	−0.80039934	−0.67011624	0.13183965	−6.0710062	1	1.27E-09	1.76E-05	−1.74158314	−1.59120117
ENSBTAG00000003955, MYO7A, protein_coding	295.849762	−0.79463621	−0.54856033	0.20508284	−3.87470846	0	0.00010675	0.03208839	−1.73463991	−1.46262541

TABLE 1 (Continued)

	baseMean	log2FoldChange	shrunkenlfc	lfcSE	stat	filter	*p* value	padj	Fold change	Shrunken Fold change
ENSBTAG00000007763, SLC1A4, protein_coding	731.552183	−0.76493065	−0.51011009	0.20801395	−3.67730452	0	0.00023571	0.0471329	−1.69928831	−1.42415887
ENSBTAG00000007156, AGAP2, protein_coding	502.509705	−0.75188674	−0.53930729	0.18867277	−3.98513651	0	6.74E-05	0.02453977	−1.68399369	−1.45327456
ENSBTAG00000016685, FMO4, protein_coding	281.168645	−0.74909699	−0.5273272	0.19717086	−3.79922766	0	0.00014515	0.03649014	−1.68074049	−1.44125659
ENSBTAG00000003100, SMTN, protein_coding	1828.20159	−0.73778949	−0.60298346	0.14279815	−5.16665997	1	2.38E-07	0.0005492	−1.66761874	−1.51885428
ENSBTAG00000010531, CYP1B1, protein_coding	302.952778	−0.73459353	−0.57562419	0.15782087	−4.65460328	0	3.25E-06	0.00374026	−1.6639286	−1.49032212
ENSBTAG00000051704, TNFRSF10D, protein_coding	2153.66879	−0.71567807	−0.57329256	0.14921157	−4.79639795	0	1.62E-06	0.00258255	−1.6422549	−1.48791547
ENSBTAG00000046476, IGSF1, protein_coding	53.4421741	−0.71226507	−0.50483777	0.19486683	−3.65513751	0	0.00025704	0.04802905	−1.63837439	−1.41896379
ENSBTAG00000001042, MXD1, protein_coding	412.83263	−0.64709909	−0.49469463	0.16738173	−3.866008	0	0.00011063	0.03254679	−1.56601615	−1.40902249
ENSBTAG00000020650, ADCYAP1, protein_coding	7138.37598	−0.63633302	−0.48586002	0.168616	−3.77385919	0	0.00016074	0.03767073	−1.5543733	−1.40042043
ENSBTAG00000001511, BCL6, protein_coding	5546.65961	−0.58499101	−0.49417875	0.12946284	−4.51860152	0	6.22E-06	0.00537952	−1.50002964	−1.40851874
ENSBTAG00000021516, GSTA1, protein_coding	5460.78137	0.61970182	0.54315932	0.11335477	5.46692312	0	4.58E-08	0.00012695	1.53655757	1.45716002
ENSBTAG00000024493, DHRS3, protein_coding	2369.08918	0.65928401	0.50356721	0.16823569	3.9188118	0	8.90E-05	0.03001018	1.57929864	1.41771467
ENSBTAG00000015086, HSD11B1, protein_coding	1492.89658	0.67415399	0.48931148	0.18314371	3.68101086	0	0.00023231	0.0471329	1.59566079	1.40377477
ENSBTAG00000003039, PSMB8, protein_coding	709.1219	0.68317143	0.52216713	0.16951175	4.03023058	0	5.57E-05	0.02082352	1.60566556	1.43611087
ENSBTAG00000021964, CDH17, protein_coding	1535.98143	0.68771286	0.58492491	0.12580542	5.46648021	0	4.59E-08	0.00012695	1.61072797	1.49996092
ENSBTAG00000014912, FMOD, protein_coding	739.722034	0.73701708	0.6215327	0.13030585	5.65605543	1	1.55E-08	0.00010708	1.66672615	1.5385088
ENSBTAG00000002333, HOPX, protein_coding	1016.20725	0.74721593	0.6000701	0.14865524	5.02650252	1	5.00E-07	0.00098667	1.67855049	1.51579021
ENSBTAG00000014291, WNT2B, protein_coding	319.903568	0.93282217	0.57235467	0.23656942	3.9431224	0	8.04E-05	0.0278018	1.9090067	1.48694849
ENSBTAG00000021880, COQ8A, protein_coding	191.22917	0.96592022	0.63707829	0.21754298	4.44013509	1	8.99E-06	0.00654253	1.95330904	1.55517646
ENSBTAG00000012543, EDA, protein_coding	19.6165426	1.2074367	0.57659555	0.31657913	3.81401229	0	0.00013673	0.0356707	2.30926974	1.49132589
ENSBTAG00000015366, SFRP4, protein_coding	886.750538	1.25803286	0.68623077	0.28545786	4.40707038	1	1.05E-05	0.00689889	2.39169408	1.60907411
ENSBTAG00000003668, RADX, protein_coding	28.5049993	1.32787195	0.59111845	0.32947259	4.0302957	1	5.57E-05	0.02082352	2.51032116	1.50641414
ENSBTAG00000022759, PAG11, protein_coding	70.901648	1.83737746	0.43593861	0.49388336	3.720266	0	0.00019901	0.04233467	3.57359827	1.35279066

(Continues)

TABLE 1 (Continued)

	baseMean	log2FoldChange	shrunkenlfc	lfcSE	stat	filter	*p* value	padj	Fold change	Shrunken Fold change
ENSBTAG00000016030, HOXD10, protein_coding	9.66888124	4.89511024	0.34181762	1.14396661	4.27906743	0	1.88E-05	0.01038009	29.7560319	1.2673523
ENSBTAG00000033330, HOXD11, protein_coding	22.7369796	5.40528012	0.2810518	1.18585902	4.5581136	0	5.16E-06	0.00475788	42.3790727	1.21508042

	baseMean	log2FoldChange	shrunkenlfc	lfcSE	stat	filter	*p* value	padj	Fold change	Shrunken fold change
ENSBTAG00000037815, HBE1, protein_coding	26.4787138	−1.91848857	−0.64987859	0.40607055	−4.72452032	1	2.31E-06	0.00297571	−3.78026813	−1.56903615
ENSBTAG00000005404, MSC, protein_coding	9.47009056	−1.68620844	−0.53638082	0.45222608	−3.72868466	0	0.00019248	0.03691229	−3.2180984	−1.45032961
ENSBTAG00000021846, CELSR3, protein_coding	28.7980484	−1.33691093	−0.70503025	0.28588494	−4.67639503	1	2.92E-06	0.00312092	−2.52609855	−1.63017884
ENSBTAG00000050986, PXDN, protein_coding	759.097847	−1.28697186	−0.63829334	0.30510584	−4.21811607	1	2.46E-05	0.01152678	−2.44015343	−1.55648679
ENSBTAG00000008111, ESYT3, protein_coding	35.4964486	−1.28597795	−0.62360821	0.31108815	−4.1338056	1	3.57E-05	0.01301056	−2.43847291	−1.54072375
ENSBTAG00000016525, ITGA1, protein_coding	100.3518	−1.22846434	−0.74425043	0.24213649	−5.07343748	1	3.91E-07	0.00135643	−2.3431744	−1.67510373
ENSBTAG00000000575, TNC, protein_coding	1942.73478	−1.18594336	−0.65829251	0.27295316	−4.34486042	1	1.39E-05	0.00974389	−2.27512113	−1.57821363
ENSBTAG00000013081, PSPH, protein_coding	529.96833	−1.04225433	−0.57189496	0.2726827	−3.82222385	0	0.00013225	0.02976424	−2.0594432	−1.48647475
ENSBTAG00000004010, PAPPA, protein_coding	705.782085	−1.03006758	−0.65821181	0.22648823	−4.54799598	1	5.42E-06	0.00480358	−2.04211991	−1.57812536
ENSBTAG00000000898,F2RL2, protein_coding	391.727257	−1.01147449	−0.57030922	0.2651496	−3.81473136	0	0.00013633	0.02976424	−2.01597045	−1.48484179
ENSBTAG00000011171, PIEZO2, protein_coding	266.685041	−0.95741882	−0.5973885	0.23464523	−4.08028251	1	4.50E-05	0.01484478	−1.94183258	−1.51297537
ENSBTAG00000005305, NTS, protein_coding	800.137496	−0.94308085	−0.56728208	0.24642762	−3.82700958	0	0.00012971	0.02976424	−1.9226296	−1.48172948
ENSBTAG00000007763, SLC1A4, protein_coding	731.552183	−0.93784076	−0.61181017	0.2203764	−4.25563146	1	2.08E-05	0.01152678	−1.91565898	−1.52817543
ENSBTAG00000049806, protein_coding	45.5574402	−0.86036732	−0.55532883	0.22431935	−3.83545739	0	0.00012533	0.02976424	−1.81550049	−1.46950354
ENSBTAG00000014788, AKAP12, protein_coding	3125.78806	−0.84079252	−0.57935931	0.20341816	−4.13332085	0	3.58E-05	0.01301056	−1.79103374	−1.49418554
ENSBTAG00000012004, TGFB3, protein_coding	492.916789	−0.82260429	−0.52851344	0.22533801	−3.65053501	0	0.00026169	0.04700897	−1.76859571	−1.44244213
ENSBTAG00000006731, SLC7A5, protein_coding	1615.61458	−0.80300952	−0.5712345	0.19264121	−4.16842025	0	3.07E-05	0.0124073	−1.74473693	−1.48579441
ENSBTAG00000013745, ITGA5, protein_coding	8536.22896	−0.69648492	−0.57619276	0.1398384	−4.98064151	0	6.34E-07	0.0014989	−1.62055156	−1.49090957
ENSBTAG00000010366, HCRTR1, protein_coding	92.8984086	−0.67396878	−0.50576093	0.1736652	−3.88085101	0	0.00010409	0.02645027	−1.59545595	−1.41987205
ENSBTAG00000006770, MTBP, protein_coding	197.974827	−0.66753843	−0.52635602	0.15623066	−4.27277469	0	1.93E-05	0.01141521	−1.58836054	−1.4402867
ENSBTAG00000022007, SAMHD1, protein_coding	507.068088	−0.65998868	−0.49619588	0.17198734	−3.83742589	0	0.00012433	0.02976424	−1.58007022	−1.41048946

TABLE 1 (Continued)

	baseMean	log2FoldChange	shrunkenlfc	lfcSE	stat	filter	*p* value	padj	Fold change	Shrunken fold change
ENSBTAG00000000446, ATP11A, protein_coding	817.397518	−0.63853304	−0.5112286	0.15082022	−4.23373624	0	2.30E-05	0.01152678	−1.55674543	−1.42526344
ENSBTAG00000021516, GSTA1, protein_coding	5460.78137	0.58634961	0.5090243	0.12023851	4.87655405	0	1.08E-06	0.00166247	1.5014429	1.42308743
ENSBTAG00000005814, PSME2, protein_coding	1461.85184	0.59167211	0.46356199	0.15837816	3.73581881	0	0.00018711	0.03637277	1.50699237	1.3789422
ENSBTAG00000037988, ZSCAN31, protein_coding	394.510381	0.59644896	0.46825745	0.15731561	3.79141629	0	0.00014979	0.03166985	1.51199038	1.38343748
ENSBTAG00000014912, FMOD, protein_coding	739.722034	0.59878705	0.50092357	0.1380527	4.33738015	0	1.44E-05	0.00974389	1.51444276	1.41511919
ENSBTAG00000003458, CDCA7, protein_coding	128.32517	0.6126092	0.47091108	0.16214237	3.7782179	0	0.00015795	0.0322565	1.52902204	1.38598445
ENSBTAG00000017810, EFHC1, protein_coding	255.040583	0.63268455	0.51540401	0.14234854	4.44461552	0	8.80E-06	0.00657635	1.55044737	1.42939437
ENSBTAG00000014878, COX7A1, protein_coding	448.645919	0.63496081	0.48829927	0.16612315	3.8222294	0	0.00013225	0.02976424	1.55289556	1.40279021
ENSBTAG00000008954, PSMB9, protein_coding	322.288285	0.64130912	0.5126677	0.15221499	4.2131797	0	2.52E-05	0.01152678	1.55974385	1.42668586
ENSBTAG00000010365, SQOR, protein_coding	297.827243	0.64827557	0.5409818	0.13217637	4.90462525	0	9.36E-07	0.00166247	1.56729371	1.45496233
ENSBTAG00000019015, IFITM3, protein_coding	17098.1904	0.66380895	0.52294932	0.15690873	4.23054199	0	2.33E-05	0.01152678	1.58425981	1.4368897
ENSBTAG00000021378,S100A13, protein_coding	410.889638	0.737533	0.54657618	0.17711502	4.16414715	0	3.13E-05	0.0124073	1.66732229	1.46061523
ENSBTAG00000007389, IFI35, protein_coding	476.508804	0.79118103	0.56433895	0.19007248	4.16252268	0	3.15E-05	0.0124073	1.7304905	1.4787098
ENSBTAG00000005182, BoLA, protein_coding	1270.66579	0.79322265	0.53057632	0.21296559	3.72465179	0	0.00019559	0.03700729	1.73294114	1.44450613
ENSBTAG00000007602, ITGA8, protein_coding	123.960196	0.82296642	0.54099383	0.22217648	3.70411138	0	0.00021213	0.03909584	1.76903969	1.45497446
ENSBTAG00000052055, PRSS35, protein_coding	926.617163	0.87588891	0.57257477	0.22005409	3.98033467	0	6.88E-05	0.02170224	1.83513846	1.48717536
ENSBTAG00000003039, PSMB8, protein_coding	709.1219	0.87604555	0.64973839	0.18024151	4.86039847	1	1.17E-06	0.00166247	1.8353377	1.56888367
ENSBTAG00000012208, protein_coding	641.996258	0.92782533	0.52508522	0.25480351	3.64133656	0	0.00027123	0.04811215	1.90240621	1.43901858
ENSBTAG00000003152, IFI27, protein_coding	12519.18	1.00530287	0.63919636	0.22516773	4.46468453	1	8.02E-06	0.00651819	2.00736487	1.55746135
ENSBTAG00000017741, HACD4, protein_coding	96.8920071	1.01382425	0.57832167	0.25558096	3.96674396	0	7.29E-05	0.02199943	2.01925659	1.49311126
ENSBTAG00000007554, IFI6, protein_coding	9514.43329	1.01384156	0.60995997	0.24571896	4.12602094	1	3.69E-05	0.01309452	2.01928083	1.52621686
ENSBTAG00000037533,C4A, protein_coding	1687.1508	1.04743914	0.62189015	0.24716276	4.23785181	1	2.26E-05	0.01152678	2.06685781	1.53889004
ENSBTAG00000004155, SPATA20, protein_coding	143.31563	1.15486135	0.81924597	0.18903435	6.10926728	1	1.00E-09	7.55E-06	2.22662923	1.76448354
ENSBTAG00000006864, protein_coding	533.66699	1.20916202	0.54071426	0.32344862	3.73834343	0	0.00018524	0.03637277	2.31203306	1.45469254
ENSBTAG00000015366, SFRP4, protein_coding	886.750538	1.57569053	0.79740628	0.30320757	5.19673877	1	2.03E-07	0.00095938	2.98078131	1.73797374

(Continues)

TABLE 1 (Continued)

	baseMean	log2FoldChange	shrunkenlfc	lfcSE	stat	filter	*p* value	padj	Fold change	Shrunken fold change
ENSBTAG00000006846, LGALS9, protein_coding	189.319423	1.57652444	0.53710214	0.41616931	3.78818044	0	0.00015175	0.03166985	2.98250475	1.45105493
ENSBTAG00000020203, TMEM151A, protein_coding	44.2503514	1.8064424	0.61919315	0.41960817	4.30506965	1	1.67E-05	0.0103706	3.4977869	1.5360159
ENSBTAG00000040244, APOL3, protein_coding	47.3460324	2.10452986	0.5057058	0.53922484	3.90288007	0	9.51E-05	0.02549885	4.30057588	1.4198178
ENSBTAG00000014529, GBP4, protein_coding	57.7785598	2.58915172	0.41020341	0.62389815	4.14995896	0	3.33E-05	0.01275406	6.01744781	1.32887316
	baseMean	**log2FoldChange**	**shrunkenlfc**	**lfcSE**	**stat**	**filter**	***p* value**	**padj**	**Fold change**	**Shrunken fold change**
ENSBTAG00000011538, KIF1A, protein_coding	70.20266	−2.23957319	−0.64752587	0.47159611	−4.74892212	1	2.05E-06	0.00688155	−4.72257331	−1.56647948
ENSBTAG00000005679, TMEM130, protein_coding	21.2912193	−2.0531094	−0.58276117	0.4826633	−4.25370933	0	2.10E-05	0.03312846	−4.14999442	−1.49771298
ENSBTAG00000033726, GRIP1, protein_coding	42.6648451	−1.04563585	−0.59317774	0.26370095	−3.96523354	1	7.33E-05	0.04934713	−2.06427597	−1.50856592
ENSBTAG00000007698, TMEM59L, protein_coding	445.22969	−0.83954751	−0.55161438	0.21807519	−3.8498076	0	0.00011821	0.04972235	−1.7894888	−1.46572493
ENSBTAG00000012012, CYB5A, protein_coding	912.792784	−0.75546844	−0.57766426	0.16723207	−4.51748539	0	6.26E-06	0.01684609	−1.68817965	−1.49243103
ENSBTAG00000047706, ING2, protein_coding	1370.59626	−0.73789537	−0.54506528	0.17903156	−4.12159382	0	3.76E-05	0.03376308	−1.66774113	−1.45908636
ENSBTAG00000002699, KIT, protein_coding	3268.693	−0.65390318	−0.52709465	0.14709654	−4.4454016	0	8.77E-06	0.01968028	−1.57341929	−1.44102428
ENSBTAG00000015248, PLA2G16, protein_coding	1726.79268	−0.63501221	−0.48962246	0.16425182	−3.86608937	0	0.00011059	0.04972235	−1.5529509	−1.40407739
ENSBTAG00000003081, RWDD4, protein_coding	1842.91844	−0.62907124	−0.49540946	0.15522398	−4.05266796	0	5.06E-05	0.03786511	−1.54656904	−1.4097208
ENSBTAG00000004375, ESRP2, pseudogene	66.9836549	0.79182826	0.55735351	0.20436503	3.87457796	0	0.00010681	0.04972235	1.73126703	1.47156729
ENSBTAG00000004155, SPATA20, protein_coding	143.31563	0.79989979	0.54641291	0.19081576	4.19200067	0	2.77E-05	0.03312846	1.74098019	1.46044995
ENSBTAG00000011131, NMUR2, protein_coding	302.704748	0.84025472	0.54728294	0.21787477	3.85659483	0	0.00011498	0.04972235	1.79036621	1.46133095
ENSBTAG00000003955, MYO7A, protein_coding	295.849762	0.90394908	0.60207688	0.21824976	4.14181022	1	3.45E-05	0.03312846	1.87118095	1.51790014
ENSBTAG00000054774, processed_pseudogene	325.949244	1.18039991	0.5864884	0.28826976	4.09477533	1	4.23E-05	0.03554937	2.26639593	1.50158734
ENSBTAG00000049042,, protein_coding	22.5892647	1.79384363	0.56725143	0.45930221	3.90558458	0	9.40E-05	0.04972235	3.46737442	1.48169801

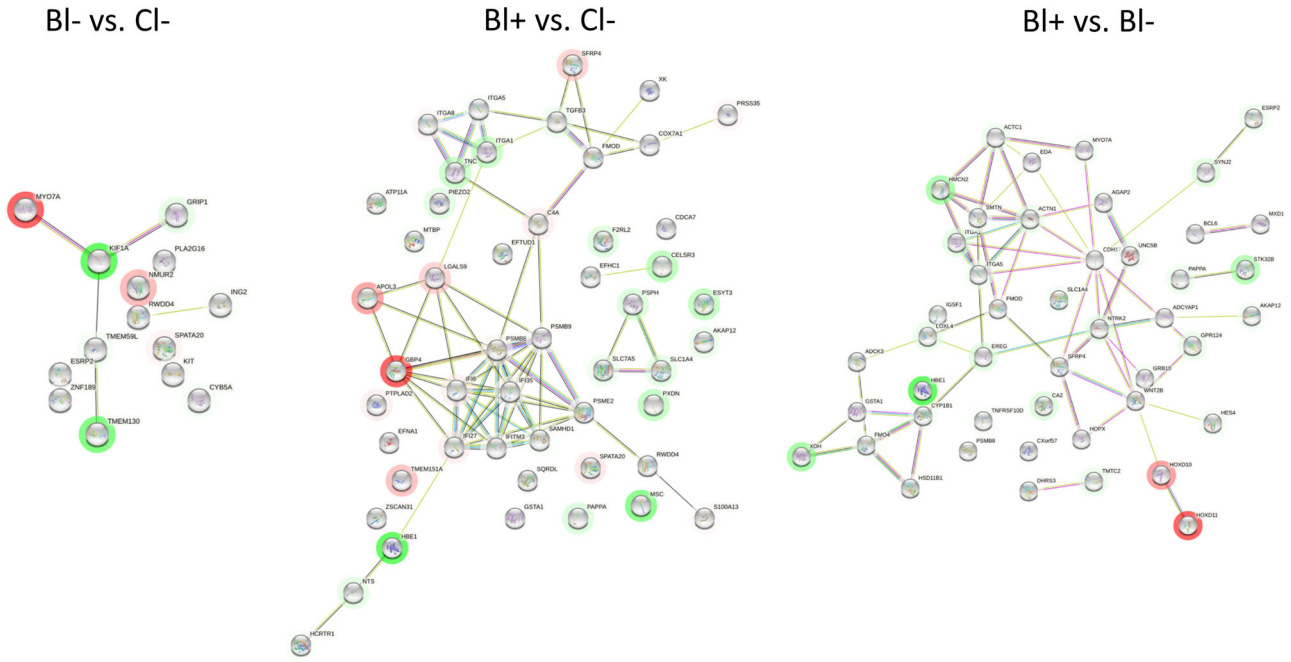

FIGURE 2 Interaction networks obtained from the DEGs at a *p* adjusted value <0.05 and fold change >1.5 at the three comparisons (from left to right Bl− vs. Cl−, Bl+ vs. Cl− and Bl+ vs. Bl−) using STRING. The color of edges and lines represents different types of evidence for protein-to-protein interaction: red for fusion evidence, green for neighborhood evidence, blue for co-occurrence evidence, purple for experimental evidence, yellow for textmining evidence, light blue for database evidence and black for coexpression evidence. DEG, differentially expressed genes.

FIGURE 3 Relative mRNA abundance of nine genes common to the comparisons Bl+ versus Bl− and Bl+ versus Cl− determined by qPCR. Mean ± standard error of the mean. Different letters indicate significant differences based on ANOVA ($p < 0.05$). ANOVA, analysis of variance; mRNA, messenger RNA.

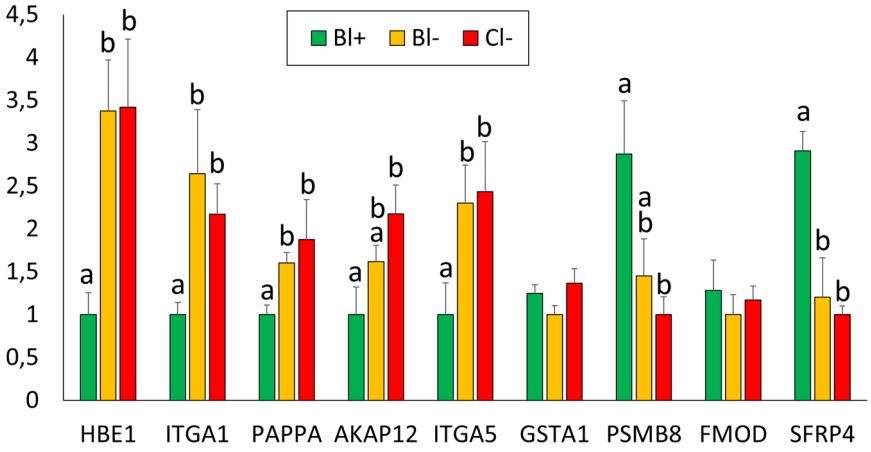

player involved in oocyte competence, as two of the genes validated by qPCR (Integrin Subunit Alpha 1 and 5, *ITGA1* and *ITGA5*) were downregulated in cumulus cells from oocytes developing to blastocysts (Bl+) compared to other groups, and enrichment analysis of biological annotations also highlighted "integrin domain superfamily" in both Bl+ versus Bl− and Bl+ versus Cl− comparisons. Integrin-mediated cell adhesions provide dynamic links between the extracellular matrix and the cytoskeleton and, in the context of oocyte maturation, they control both cumulus cell expansion and luteinization, increasing their expression during cumulus expansion (Kitasaka et al., 2018) and ovulation (Wissing et al., 2014). In this sense, the negative correlation between integrin expression in cumulus cells and oocyte quality may indicate that competent IVM oocytes may achieve cumulus cell expansion earlier or to a greater extend, thereby resuming the expression of the integrins required for expansion before the end of IVM. In agreement with this hypothesis, cumulus expansion intensity is positively linked to embryo development (Qian et al., 2003), and *ITGA5* was found to be upregulated in cumulus cells from rhesus monkey oocytes matured in vitro compared to those matured in vivo (Lee et al., 2011).

Other genes downregulated in cumulus cells from competent oocytes include *HBE1*, *PAPPA*, and *AKAP12*. *HBE1* encodes for Epsilon 1 subunit of hemoglobin. Hemoglobin has been reported to be expressed by mouse preimplantation embryos where it was

TABLE 2 Details of primers used for qPCR

Gene	Primer sequence (5′–3′)	Fragment size (bp)	GenBank accession no.
PPIA	CGGGATTTATGTGCCAGGGT	218	NM_178320.2
	CCAAAGTACCACGTGCTTGC		
HBE1	CTGAGTGAGCTGCACTGTGA	219	NM_001110507.1
	AGGCACTGGGGACACAAAAT		
ITGA1	AGGGCAGAACTTCAGAGTGA	100	XM_024981466.1
	TGCCTGGTAGCCCATCTTTG		
PAPPA	CAAGGAGGGCAAGTGGAACA	234	XM_024996354.1
	AGGCACATGAGCTCACACAG		
AKAP12	AAAACCCGAACCCACGGAAT	154	XM_024997063.1
	TGAGCAGTTGACACGTCTGT		
ITGA5	AGTGGATCAAGGCAGAAGGC	197	NM_001166500.1
	GAGGAATCAGGCATCGGAGG		
GSTA1	GTGCCCACCTGCTGAAAAAG	202	NM_001078149.1
	GAAGTTGGCCAAAAGGCTGG		
PSMB8	TGGCCTTCAAGTTCCAGCAT	210	NM_001040480.1
	TACGCTCCCCATTCCTCAGA		
FMOD	GGCCTGGCCTCAAATACCTT	153	NM_174058.2
	GCAGAAGCTGCTGATGGAGA		
SFRP4	CCACACATCCTGCCTCATCA	180	NM_001075764.1
	TGCTGTTCGCTTCTTGTCCT		

suggested to play a role on embryonic oxygen regulation (Lim et al., 2019). As oxidative stress exerts a negative impact on oocyte competence (Bennemann et al., 2018; Bermejo-Alvarez et al., 2010), the lower expression of *HBE1* in cumulus cells from competent oocytes may indicate a reduced exposure to oxygen during folliculogenesis, before IVM, or a higher ability to deal with oxidative stress during IVM. Pregnancy-associated plasma protein-A (PAPPA) regulates ovarian follicle dominance by degrading IGFBP-4 in preovulatory follicles of several species, including cattle (Mazerbourg et al., 2001; Rivera & Fortune, 2001). Similarly to integrins, *PAPPA* expression increases during bovine folliculogenesis (Mazerbourg et al., 2001) and thereby the lower expression in cumulus cells from more competent oocytes may indicate that they have attained full developmental competence by the end of IVM. Finally, A-Kinase Anchoring Protein 12 (*AKAP12*) overexpression in the cumulus cells from mice lacking estrogen receptor beta has been suggested to contribute to the sequestration of PKA regulatory units, leading to reduced cAMP levels (Binder et al., 2013). In this perspective, the higher expression of *AKAP12* in cumulus cells from incompetent bovine oocytes may be linked to reduced cAMP, diminishing the odds to progress to the blastocyst stage (Luciano et al., 1999).

Other genes (*SFRP4*, *PSMB8*, *FMOD*, and *GSTA1*) were upregulated in cumulus cells from competent oocytes, although the differences in *FMOD* and *GSTA1* expression were not confirmed by qPCR. Secreted Frizzled Related Protein 4 (SFRP4) inhibits Wnt signaling, a pathway known to play multiple functions during folliculogenesis (Hernandez Gifford, 2015). The role of SFRP4 during folliculogenesis remain under debate, as its ablation in mice has been reported to increase (Zamberlam et al., 2019) or decrease (Christov et al., 2011) litter size, and whereas mRNA content in human cumulus cells was positively associated with in vivo meiotic progression (Devjak et al., 2012), protein content in human follicular fluid has been negatively associated with in vitro meiotic progression (Pla et al., 2021). The differences between studies may be linked to the different hormonal environment of in vitro and in vivo maturation, as *SFRP4* expression is modulated by LH in a species-specific manner (Maman et al., 2011). The agreement between our findings and those obtained in human IVM (Pla et al., 2021) suggest that, in contrast to rodents, bovine and humans may share a similar regulation of *SFRP4*, although dedicated experiments would be required to test this hypothesis. Proteasome 20 S subunit beta 8 (PSMB8) is a component of the proteasome, which modulates oocyte meiotic maturation (Huo et al., 2004). In agreement with the positive association between *PSMB8* expression and oocyte quality observed in bovine cumulus cells, the expression level of its antisense (PSMB8-AS1) was higher in cumulus cells from old versus young women (Bouckenheimer et al., 2018). Finally, although qPCR data did not detect significant differences between groups in glutathione S-Transferase Alpha 1

(*GSTA1*) expression, the positive association between *GSTA1* expression and oocyte quality observed by RNA-seq is consistent with previous findings. GSTA1 catalyzes the conjugation of glutathione to molecules such as prostaglandins A2 and J2 and it has been found to display steroid isomerase activity in bovine (Raffalli-Mathieu et al., 2007). *GSTA1* expression in bovine cumulus cells increases following FSH and/or phorbol myristate addition to IVM media, which resulted in improved rates of blastocyst development (Assidi et al., 2008). *GSTA1* transcript abundance is also higher in cumulus cells from in vivo matured bovine oocytes compared to IVM counterparts (Salhab et al., 2013) and in bovine oocytes selected by Brilliant Cresyl Blue staining (Janowski et al., 2012).

In conclusion, the transcriptome of bovine cumulus cells from COCs exhibiting different developmental competence following individual IVP differs in a small subset of genes involved in critical biological functions such as integrin-mediated cell adhesion, oxygen availability, IGF and Wnt signaling or PKA pathway. Such biological functions are required during folliculogenesis to attain full oocyte competence, thereby highlighting specific processes altered in incompetent IVM bovine oocytes.

4 | MATERIALS AND METHODS

4.1 | Individual IVP and collection of cumulus cells samples

Bovine embryos were produced from slaughterhouse ovaries following conventional protocols (Lamas-Toranzo et al., 2020), adapted to individual embryo production. Bovine ovaries were transported at 35–37°C from a local slaughterhouse to the laboratory. COCs were aspirated from surface visible antral follicles (2–8 mm) and selected using conventional morphological criteria (Hawk & Wall, 1994). Individual in vitro production (iIVP) was required to determine the developmental ability of each oocyte. COCs were matured individually in 40 µl drops of TCM-199 supplemented with 10% fetal calf serum (FCS) and 10 ng/ml epidermal growth factor covered under mineral oil at 39°C and 5% CO_2 in air with humidified atmosphere for 24 h. Following maturation, the cumulus cells from each individual COC were removed by pipetting in medium supplemented with 0.1% hyaluronidase. Cumulus cells were collected from the media by centrifugation at 1500 rpm for 5 min, snap frozen in liquid nitrogen and stored at −80°C until analysis. Denuded oocytes were individually inseminated in 40 µl drops of TALP medium covered under mineral oil and containing 1×10^6 frozen-thawed bull spermatozoa/ml. After 20 h of gamete coincubation, presumptive zygotes were cultured individually in 10 µl drops of synthetic oviduct fluid medium supplemented with 5% FCS at 39°C and in a 5% CO_2 and 5% O_2 water-saturated atmosphere. Embryo development was assessed for each individual oocyte at 48 h postinsemination (cleavage, at least 4-cells) and at day 8 postinsemination (blastocyst formation).

4.2 | Transcriptional analysis

RNA extraction was performed on 4 (CI−) or 5 (BI− and BI+) samples per group each of which was composed of cumulus cells obtained from 10 individual COCs. Individual samples (i.e., 40 CI−, 50 BI−, and 50 BI+) were collected from 7 independent replicates. The rationale behind analyzing three experimental groups was to double-check for the correlation between transcriptional change and developmental competence; for instance a "positive marker" for oocyte competence should be upregulated in BI+ versus BI− but also between BI+ and CI−. Total RNA was extracted using MagMAX *mir*Vana Total Isolation Kit (Applied Biosystems) following the manufacturer's instruction with minor modifications. Briefly 200 µl of Lysis Binding Mix were added to the sample, followed by gentle pipetting and 5 min incubation at room temperature. Then 20 µl of Binding Beads Mix were added and shaken gently for 5 min. Beads-mRNA complexes were washed once in each Wash Solution 1 and 2. Following the washing step, samples were treated with 50 µl of Turbo DNAse treatment, 50 µl of Rebinding Buffer and 100 µl of Isopropanol were added to the sample and mixed gently. Finally, following a double wash in Wash Solution 2, total RNA was eluted in 20 µl of Elution Buffer and stored at −80°C until analysis.

RNA samples were quantified by Qubit RNA BR Assay (Thermo Fisher Scientific) and RNA integrity was estimated by using RNA 6000 Nano Bioanalyzer 2100 Assay (Agilent). RNA amount oscillated between 0.285 and 0.676 µg and RIN values between 8 and 9.2. RNA-seq libraries were prepared with KAPA Stranded mRNA-Seq Illumina Platforms Kit (Roche) following the manufacturer's recommendations. Briefly, 50–100 ng of total RNA was used for the poly-A fraction enrichment with oligo-dT magnetic beads, following the mRNA fragmentation. The strand specificity was achieved during the second strand synthesis performed in the presence of dUTP instead of dTTP. The blunt-end double stranded cDNA was 3′ adenylated and Illumina platform compatible adaptors with unique dual indexes and unique molecular identifiers (Integrated DNA Technologies) were ligated. The ligation product was enriched with 15 PCR cycles and the final library was validated on an Agilent 2100 Bioanalyzer with the DNA 7500 assay.

The libraries were sequenced on a HiSeq. 4000 system (Illumina) with a read length of 2 × 76 bp + 8 bp + 8 bp using the HiSeq. 4000 SBS kit (Illumina) obtaining >30 M reads/sample. Image analysis, base calling and quality scoring of the run were processed using the manufacturer's software Real Time Analysis (RTA 2.7.7). Differential expression was analysed by DESeq. 2 software obtaining raw p values, adjusted *p* values, raw fold changes and shrunken fold changes for all genes detected. Enrichment in biological annotations and a network of biological interactions for each of the three comparisons were performed on differentially expressed genes (DEGs) with an adjusted *p* value <0.05 and fold change >1.5 using STRING (v11; Szklarczyk et al., 2019) through the package "STRINGdb" in R (v4.0.4). Only enriched terms with FDR < 0.05 calculated by the Benjamini-Hochberg procedure were selected.

RNA-seq validation was performed on independently retro-transcribed cDNA obtained from the RNA samples mentioned above using qScript cDNA Supermix (Quantabiosciences, containing a blend of random and oligo dT primers optimized to deliver unbiased representation of 5′ and 3′ sequences) in a 20 µl final volume. Relative mRNA abundance of 9 selected DEGs was analyzed in 4 (CI−) or 5 (BI− and BI+) samples by qPCR as previously described (Lamas-Toranzo et al., 2018) using specific primers detailed in Table 2. Experiments were conducted to contrast the relative levels of each transcript and the housekeeping gene *PPIA* in each sample. cDNA was diluted to 55 µl in 10 mM Tris-HCl (pH 7.5) and qPCR was performed in duplicate by adding a 2 µl aliquot of diluted cDNA to the PCR mix containing the specific primers for each DEG. PCR efficiencies were optimized to achieve efficiencies close to 1 and then the comparative cycle threshold (Cq) method was used to quantify expression levels as described in (Schmittgen & Livak, 2008). As primers were designed using the same annealing parameters, all qPCRs were performed using the same cycling conditions: 40 cycles of 94°C 15 s, 56°C 30 s, and 72°C 20 s followed by a final melting assay to assess product identity. Cq value was taken in the log-linear phase of the reaction, and ΔCq value was determined by substracting the *PPIA* Cq value for each sample from each gene Cq value of the sample. Calculation of ΔΔCq involved using the highest sample ΔCq value (i.e., the sample with the lowest target expression) as an arbitrary constant to subtract from all other ΔCq sample values. Fold changes in the relative gene expression of the target were determined using the formula $2^{-\Delta\Delta Cq}$. qPCR data were analysed by one way analysis of variance using the statistical software Sigma Stat (Jandel Scientific).

ACKNOWLEDGMENTS

The authors want to acknowledge “Kildare Chilling Company” for kindly providing bovine ovaries to conduct the experiments. This work was funded by the projects IND2017/BIO-7748 from Madrid Region Government and AGL2017-84908-R and PID2020-117501RB-I00 by the Spanish Ministry of Economy, Industry and Competitiveness (MINECO). AMM was funded by project IND2017/BIO-7748 and ILT by a FPI fellowship by MINECO.

CONFLICTS OF INTEREST

The authors declare no conflicts of interest.

DATA AVAILABILITY STATEMENT

The data that support the findings of this study are available from the corresponding author upon reasonable request.

PEER REVIEW

The peer review history for this article is available at https://publons.com/publon/10.1002/mrd.23631

REFERENCES

Assidi, M., Dieleman, S. J., & Sirard, M. A. (2010). Cumulus cell gene expression following the LH surge in bovine preovulatory follicles: potential early markers of oocyte competence. *Reproduction*, *140*(6), 835–852. https://doi.org/10.1530/REP-10-0248

Assidi, M., Dufort, I., Ali, A., Hamel, M., Algriany, O., Dielemann, S., & Sirard, M. A. (2008). Identification of potential markers of oocyte competence expressed in bovine cumulus cells matured with follicle-stimulating hormone and/or phorbol myristate acetate in vitro. *Biology of Reproduction*, *79*(2), 209–222.

Baruselli, P. S., Ferreira, R. M., Vieira, L. M., Souza, A. H., Bo, G. A., & Rodrigues, C. A. (2020). Use of embryo transfer to alleviate infertility caused by heat stress. *Theriogenology*, *155*, 1–11. https://doi.org/10.1016/j.theriogenology.2020.04.028

Bennemann, J., Grothmann, H., & Wrenzycki, C. (2018). Reduced oxygen concentration during in vitro oocyte maturation alters global DNA methylation in the maternal pronucleus of subsequent zygotes in cattle. *Molecular Reproduction and Development*, *85*(11), 849–857. https://doi.org/10.1002/mrd.23073

Bermejo-Alvarez, P., Lonergan, P., Rizos, D., & Gutierrez-Adan, A. (2010). Low oxygen tension during IVM improves bovine oocyte competence and enhances anaerobic glycolysis. *Reproductive BioMedicine Online*, *20*(3), 341–349.

Bettegowda, A., Patel, O. V., Lee, K. B., Park, K. E., Salem, M., Yao, J., Ireland, J. J., & Smith, G. W. (2008). Identification of novel bovine cumulus cell molecular markers predictive of oocyte competence: Functional and diagnostic implications. *Biology of Reproduction*, *79*(2), 301–309. https://doi.org/10.1095/biolreprod.107.067223

Binder, A. K., Rodriguez, K. F., Hamilton, K. J., Stockton, P. S., Reed, C. E., & Korach, K. S. (2013). The absence of ER-beta results in altered gene expression in ovarian granulosa cells isolated from in vivo preovulatory follicles. *Endocrinology*, *154*(6), 2174–2187. https://doi.org/10.1210/en.2012-2256

Bouckenheimer, J., Fauque, P., Lecellier, C. H., Bruno, C., Commes, T., Lemaître, J. M., De Vos, J., & Assou, S. (2018). Differential long non-coding RNA expression profiles in human oocytes and cumulus cells. *Scientific Reports*, *8*(1), 2202. https://doi.org/10.1038/s41598-018-20727-0

Bunel, A., Jorssen, E. P., Merckx, E., Leroy, J. L., Bols, P. E., & Sirard, M. A. (2015). Individual bovine in vitro embryo production and cumulus cell transcriptomic analysis to distinguish cumulus-oocyte complexes with high or low developmental potential. *Theriogenology*, *83*(2), 228–237. https://doi.org/10.1016/j.theriogenology.2014.09.019

Bunel, A., Nivet, A. L., Blondin, P., Vigneault, C., Richard, F. J., & Sirard, M. A. (2014). Cumulus cell gene expression associated with pre-ovulatory acquisition of developmental competence in bovine oocytes. *Reproduction, Fertility, and Development*, *26*(6), 855–865. https://doi.org/10.1071/RD13061

Christov, M., Koren, S., Yuan, Q., Baron, R., & Lanske, B. (2011). Genetic ablation of sfrp4 in mice does not affect serum phosphate homeostasis. *Endocrinology*, *152*(5), 2031–2036. https://doi.org/10.1210/en.2010-1351

Devjak, R., Fon Tacer, K., Juvan, P., Virant Klun, I., Rozman, D., & Vrtacnik Bokal, E. (2012). Cumulus cells gene expression profiling in terms of oocyte maturity in controlled ovarian hyperstimulation using GnRH agonist or GnRH antagonist. *PLoS One*, *7*(10), e47106. https://doi.org/10.1371/journal.pone.0047106

Dieleman, S. J., Hendriksen, P. J., Viuff, D., Thomsen, P. D., Hyttel, P., Knijn, H. M., Wrenzycki, C., Kruip, T. A., Niemann, H., Gadella, B. M., Bevers, M. M., & Vos, P. L. (2002). Effects of in vivo prematuration and in vivo final maturation on developmental capacity and quality of pre-implantation embryos. *Theriogenology*, *57*(1), 5–20. https://doi.org/10.1016/s0093-691x(01)00655-0

Ferre, L. B., Kjelland, M. E., Strobech, L. B., Hyttel, P., Mermillod, P., & Ross, P. J. (2020). Review: Recent advances in bovine in vitro embryo production: reproductive biotechnology history and methods. *Animal*, *14*(5), 991–1004. https://doi.org/10.1017/S1751731119002775

Hawk, H. W., & Wall, R. J. (1994). Improved yields of bovine blastocysts from in vitro-produced oocytes. I. Selection of oocytes and zygotes. *Theriogenology*, 41(8), 1571–1583. https://doi.org/10.1016/0093-691x(94)90822-z

Hernandez Gifford, J. A. (2015). The role of WNT signaling in adult ovarian folliculogenesis. *Reproduction*, *150*(4), R137–R148. https://doi.org/10.1530/REP-14-0685

Huo, L. J., Fan, H. Y., Zhong, Z. S., Chen, D. Y., Schatten, H., & Sun, Q. Y. (2004). Ubiquitin-proteasome pathway modulates mouse oocyte meiotic maturation and fertilization via regulation of MAPK cascade and cyclin B1 degradation. *Mechanisms in Developent*, *121*(10), 1275–1287. https://doi.org/10.1016/j.mod.2004.05.007

Janowski, D., Salilew-Wondim, D., Torner, H., Tesfaye, D., Ghanem, N., Tomek, W., El-Sayed, A., Schellander, K., & Hölker, M. (2012). Incidence of apoptosis and transcript abundance in bovine follicular cells is associated with the quality of the enclosed oocyte. *Theriogenology*, *78*(3), e651–e655. https://doi.org/10.1016/j.theriogenology.2012.03.012

Kitasaka, H., Kawai, T., Hoque, S. A. M., Umehara, T., Fujita, Y., & Shimada, M. (2018). Inductions of granulosa cell luteinization and cumulus expansion are dependent on the fibronectin-integrin pathway during ovulation process in mice. *PLoS One*, *13*(2), e0192458. https://doi.org/10.1371/journal.pone.0192458

Kussano, N. R., Leme, L. O., Guimaraes, A. L., Franco, M. M., & Dode, M. A. (2016). Molecular markers for oocyte competence in bovine cumulus cells. *Theriogenology*, *85*(6), 1167–1176. https://doi.org/10.1016/j.theriogenology.2015.11.033

Lamas-Toranzo, I., Galiano-Cogolludo, B., Cornudella-Ardiaca, F., Cobos-Figueroa, J., Ousinde, O., & Bermejo-Álvarez, P. (2019). Strategies to reduce genetic mosaicism following CRISPR-mediated genome edition in bovine embryos. *Scientific Reports*, *9*(1), 14900. https://doi.org/10.1038/s41598-019-51366-8

Lamas-Toranzo, I., Martinez-Moro, A. E. O. C., Millan-Blanca, G., Sanchez, J. M., Lonergan, P., & Bermejo-Alvarez, P. (2020). RS-1 enhances CRISPR-mediated targeted knock-in in bovine embryos. *Molecular Reproduction and Development*, *87*(5), 542–549. https://doi.org/10.1002/mrd.23341

Lamas-Toranzo, I., Pericuesta, E., & Bermejo-Alvarez, P. (2018). Mitochondrial and metabolic adjustments during the final phase of follicular development prior to IVM of bovine oocytes. *Theriogenology*, *119*, 156–162. https://doi.org/10.1016/j.theriogenology.2018.07.007

Lee, Y. S., VandeVoort, C. A., Gaughan, J. P., Midic, U., Obradovic, Z., & Latham, K. E. (2011). Extensive effects of in vitro oocyte maturation on rhesus monkey cumulus cell transcriptome. *American Journal of Physiology, Endocrinoly and Metabolism*, *301*(1), E196–E209. https://doi.org/10.1152/ajpendo.00686.2010

van de Leemput, E. E., Vos, P. L., Zeinstra, E. C., Bevers, M. M., van der Weijden, G. C., & Dieleman, S. J. (1999). Improved in vitro embryo development using in vivo matured oocytes from heifers superovulated with a controlled preovulatory LH surge. *Theriogenology*, *52*(2), 335–349. https://doi.org/10.1016/s0093-691x(99)00133-8

Lim, M., Brown, H. M., Kind, K. L., Breen, J., Anastasi, M. R., Ritter, L. J., Tregoweth, E. K., Dinh, D. T., Thompson, J. G., & Dunning, K. R. (2019). Haemoglobin expression in in vivo murine preimplantation embryos suggests a role in oxygen-regulated gene expression. *Reproduction, Fertility, and Development*, *31*(4), 724–734. https://doi.org/10.1071/RD17321

Luciano, A. M., Pocar, P., Milanesi, E., Modina, S., Rieger, D., Lauria, A., & Gandolfi, F. (1999). Effect of different levels of intracellular cAMP on the in vitro maturation of cattle oocytes and their subsequent development following in vitro fertilization. *Molecular Reproduction and Development*, *54*(1), 86–91. https://doi.org/10.1002/(SICI)1098-2795(199909)54:1<86::AID-MRD13>3.0.CO;2-C

Maman, E., Yung, Y., Cohen, B., Konopnicki, S., Dal Canto, M., Fadini, R., Kanety, H., Kedem, A., Dor, J., & Hourvitz, A. (2011). Expression and regulation of sFRP family members in human granulosa cells. *Molecular Human Reproduction*, *17*(7), 399–404. https://doi.org/10.1093/molehr/gar010

Mazerbourg, S., Overgaard, M. T., Oxvig, C., Christiansen, M., Conover, C. A., Laurendeau, I., Vidaud, M., Tosser-Klopp, G., Zapf, J., & Monget, P. (2001). Pregnancy-associated plasma protein-A (PAPP-A) in ovine, bovine, porcine, and equine ovarian follicles: Involvement in IGF binding protein-4 proteolytic degradation and mRNA expression during follicular development. *Endocrinology*, *142*(12), 5243–5253. https://doi.org/10.1210/endo.142.12.8517

Melo, E. O., Cordeiro, D. M., Pellegrino, R., Wei, Z., Daye, Z. J., Nishimura, R. C., & Dode, M. A. (2017). Identification of molecular markers for oocyte competence in bovine cumulus cells. *Animal Genetics*, *48*(1), 19–29. https://doi.org/10.1111/age.12496

Pla, I., Sanchez, A., Pors, S. E., Pawlowski, K., Appelqvist, R., Sahlin, K. B., Poulsen, L. C., Marko-Varga, G., Andersen, C. Y., & Malm, J. (2021). Proteome of fluid from human ovarian small antral follicles reveals insights in folliculogenesis and oocyte maturation. *Human Reproduction*, *36*(3), 756–770. https://doi.org/10.1093/humrep/deaa335

Qian, Y., Shi, W. Q., Ding, J. T., Sha, J. H., & Fan, B. Q. (2003). Predictive value of the area of expanded cumulus mass on development of porcine oocytes matured and fertilized in vitro. *Journal of Reproduction Development*, *49*(2), 167–174. https://doi.org/10.1262/jrd.49.167

Raffalli-Mathieu, F., Persson, D., & Mannervik, B. (2007). Differences between bovine and human steroid double-bond isomerase activities of alpha-class glutathione transferases selectively expressed in steroidogenic tissues. *Biochimica et Biophysica Acta*, *1770*(1), 130–136. https://doi.org/10.1016/j.bbagen.2006.06.015

Rivera, G. M., & Fortune, J. E. (2001). Development of codominant follicles in cattle is associated with a follicle-stimulating hormone-dependent insulin-like growth factor binding protein-4 protease. *Biology of Reproduction*, *65*(1), 112–118. https://doi.org/10.1095/biolreprod65.1.112

Rizos, D., Lonergan, P., Ward, F., Duffy, P., & Boland, M. (2002). Consequences of bovine maturation, fertilization or early embryo development in vitro versus in vivo: Implications for blastocyst yield and blastocyst quality. *Molecular Reproduction and Development*, *61*, 234–248.

Salhab, M., Dhorne-Pollet, S., Auclair, S., Guyader-Joly, C., Brisard, D., Dalbies-Tran, R., Dupont, J., Ponsart, C., Mermillod, P., & Uzbekova, S. (2013). In vitro maturation of oocytes alters gene expression and signaling pathways in bovine cumulus cells. *Molecular Reproduction and Development*, *80*(2), 166–182. https://doi.org/10.1002/mrd.22148

Schmittgen, T. D., & Livak, K. J. (2008). Analyzing real-time PCR data by the comparative C(T) method. *Nature Protocols*, *3*(6), 1101–1108.

Szklarczyk, D., Gable, A. L., Lyon, D., Junge, A., Wyder, S., Huerta-Cepas, J., Simonovic, M., Doncheva, N. T., Morris, J. H., Bork, P., Jensen, L. J., & Mering, C. V. (2019). STRING v11: Protein-protein association networks with increased coverage, supporting functional discovery in genome-wide experimental datasets. *Nucleic Acids Research*, *47*(D1), D607–D613. https://doi.org/10.1093/nar/gky1131

Tesfaye, D., Ghanem, N., Carter, F., Fair, T., Sirard, M. A., Hoelker, M., Schellander, K., & Lonergan, P. (2009). Gene expression profile of cumulus cells derived from cumulus-oocyte complexes matured either in vivo or in vitro. *Reproduction, Fertility, and Development*, *21*(3), 451–461. https://doi.org/10.1071/rd08190

Wissing, M. L., Kristensen, S. G., Andersen, C. Y., Mikkelsen, A. L., Host, T., Borup, R., & Grondahl, M. L. (2014). Identification of new ovulation-related genes in humans by comparing the transcriptome of granulosa cells before and after ovulation triggering in the same controlled ovarian stimulation cycle. *Human Reproduction*, *29*(5), 997–1010. https://doi.org/10.1093/humrep/deu008

Zamberlam, G., Lapointe, E., Abedini, A., Rico, C., Godin, P., Paquet, M., Demayo, F. J., & Boerboom, D. (2019). SFRP4 is a negative regulator of ovarian follicle development and female fertility. *Endocrinology*, *160*(7), 1561–1572. https://doi.org/10.1210/en.2019-00212

How to cite this article: Martínez-Moro, Á., González-Brusi, L., Lamas-Toranzo, I., O'Callaghan, E., Esteve-Codina, A., Lonergan, P., & Bermejo-Álvarez, P. (2022). RNA-sequencing reveals genes linked with oocyte developmental potential in bovine cumulus cells. *Molecular Reproduction and Development*, 89, 399–412. https://doi.org/10.1002/mrd.23631